Elastic and vibrational properties of pseudomorphic FeSi films

H. von Känel, M. Mendik,* K. A. Mäder,† N. Onda, S. Goncalves-Conto, and C. Schwarz
Laboratorium für Festkörperphysik, Eidgenössische Technische Hochschule Zürich, CH-8093 Zürich, Switzerland

G. Malegori and L. Miglio
Dipartimento di Fisica dell'Università, via Celoria 16, I-20133 Milano, Italy

F. Marabelli
Dipartimento di Fisica, "Alessandro Volta," via Bassi 6, I-27100 Pavia, Italy
(Received 29 September 1993; revised manuscript received 24 March 1994)

We analyze the structural, vibrational, and elastic properties of epitaxial novel FeSi films on Si(111) in the CsCl structure by Rutherford-backscattering spectrometry, x-ray-diffraction, infrared transmittance/reflectance, and Brillouin-light-scattering measurements. By comparing our results for different film thicknesses and by interpreting them on the basis of semiempirical total-energy calculations, we are able to relate the changes in vibrational properties with the progressive strain relaxation as a function of sample thickness. For the thickest film (890 Å) we obtain indications that a structural transition to the (bulk) ϵ phase is about to take place.

I. INTRODUCTION

Very recently, the successful synthesis of a novel FeSi phase with the CsCl structure has been reported by three of us:[1] epitaxial films as thick as several hundred Å were grown by molecular-beam epitaxy (MBE). We are now interested in improving the understanding of the structural, elastic, and vibrational properties of this phase. The main question to be addressed in this paper is how these properties depend on the thickness of the films. Rutherford-backscattering spectrometry (RBS) and x-ray-diffraction (XRD) data indicate increasing strain relaxation with film thickness, which is likely to affect both the optical vibrations and the elastic constants. Infrared and Brillouin measurements on different samples are analyzed and compared to semiempirical total-energy calculations, fitted onto *ab initio* results of the electronic structure. In particular, we present below a summary of the sample characteristics (Sec. II), the description of the experimental measurements (Secs. III and IV), a brief outline of the calculation procedure (Sec. V), and a comparative discussion of our results (Sec. VI).

II. GROWTH AND SAMPLE CHARACTERISTICS

The FeSi films were grown on Si(111) in a two-step procedure. Either two monolayers of pure Fe or an ultrathin $FeSi_2$ template (10 Å) were deposited first, followed by molecular-beam epitaxy up to the desired thickness with the substrate maintained at room temperature (RT). Details of the procedure can be found in Ref. 2.

Films grown in this fashion exhibited a 1×1 pattern in reflection high-energy electron diffraction (RHEED) and intense Kikuchi bands typical for a cubic structure with the [111] axis aligned with that of Si. The lateral orientation of the silicide was determined to be of type *B*, i.e., the films are totaled by 180 degrees around the Si[111] surface normal. The CsCl structure was assigned to this new, epitaxially stabilized[3] (or *pseudomorphic*[4]) monosilicide phase on the basis of consistent diffraction information obtained by transmission electron microscopy (TEM), XRD, and RHEED. When the diffraction patterns or Kichuchi bands are indexed according to a cubic unit cell with the Si lattice parameter a_{Si}, all reflections with odd order indices are found to be absent, as expected for the CsCl structure with a lattice parameter close to $a_{Si}/2$.[1] The thickest sample that we obtain with such characteristics corresponds to 890 Å, since for larger thickness the ϵ phase is always generated. XRD and RBS channeling through off-normal channeling minima of substrate and overlayer showed that the films are under a homogeneous compressive strain up to a critical thickness h_c of the order of 70 Å,[5] at RT. Actually, the

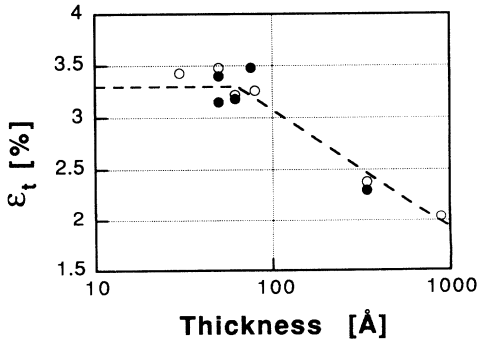

FIG. 1. Trigonal strain $\epsilon_t=\epsilon_{\parallel}-\epsilon_{\perp}$ as a function of film thickness as measured by x-ray diffraction (open symbols) and by Rutherford-backscattering channeling (filled symbols). The dashed-dotted curve is a guide to the eye.

biaxial stress originates from the lattice mismatch between Si and FeSi, since the lattice constant of the latter, $a_{FeSi}=2.77$ Å, exceeds half the Si lattice constant by $\sim 2\%$. The resulting trigonal distortion $\epsilon_t=\epsilon_{\parallel}-\epsilon_{\perp}$ of the lattice, where $\epsilon_{\parallel}$ and $\epsilon_{\perp}$ denote the strain parallel and perpendicular to the substrate, respectively, turns out to be substantial, as can be seen in Fig. 1, where ϵ_t is plotted against the film thickness h. Above ~ 70-Å biaxial strain relaxation sets in, generating a reduction of the trigonal distortion. In reality the situation is somewhat complicated by the fact that the step structure associated with the finite unintentional misorientation of the substrate may give rise to uniaxial strain relaxation of B-type oriented films, irrespective of their thickness.[2] For this reason the shift of the phonon frequencies (see below) were compared with the actual trigonal distortion ϵ_t, as determined for each individual sample, rather than taking $\epsilon_t(h)$ from the interpolated curve shown in Fig. 1.

III. INFRARED MEASUREMENTS

Transmittance and reflectance measurements in the far infrared (FIR) were performed with a Fourier transform spectrometer on several samples of different thicknesses and on a piece of Si substrate used as reference. The transmittance data were normalized to the transmittance of the Si substrate, in order to extract only the contribution from the films. This contribution can be divided into two parts: one is a large continuum due to free carriers, confirming the metallic character of FeSi(CsCl), the second is a single small absorption structure, corresponding to the transverse optical (TO) phonon of FeSi. The absolute values of the reflectance as well as those of the absorbance increase for increasing thickness of the film. In all the investigated samples both kinds of measurements yield a single absorption structure, with an intensity of a few percent, at an energy between 335 and 351 cm^{-1} (see Fig. 2). The energy of the phonon can be derived directly from the spectral position of the maximum in the absorption (or reflection) peak and the bandwidth γ from its width at half maximum (after background subtraction). The 350-Å sample exhibits a lower frequency, $\omega_0=335$ cm^{-1}, than the 62-Å sample with $\omega_0=348$ cm^{-1} and the 50-Å sample for which $\omega_0=351$ cm^{-1}. The 890-Å sample shows a peak at about 348 cm^{-1}, but some small satellite structures appear in reflectance as well as in absorbance measurements. The bandwidths do not show any clear dependence on the samples, being all of the order of 40 cm^{-1}.

The values obtained by absorbance and by reflectance agree within 1 cm^{-1} for the energies and within 5 cm^{-1} for the bandwidths. The thickest sample forms an exception, both methods yielding different line shapes (Fig. 2).

We also used a model to fit the reflectance spectra, with one Lorentzian oscillator and a Drude term describing the optical response of a layer on Si. The best fit values of the phonon energy agree very well with the ones reported above: only the frequency of the 350-Å sample lies too low (326 cm^{-1}). The γ values obtained from the fit increase for increasing film thickness, passing from about 25 cm^{-1} for the 50-Å sample to 60 cm^{-1} for the 350-Å sample. Again the 890-Å sample, where a poor fit was obtained, does not follow this trend, suggesting that some effect other than strain relaxation might have occurred.

For the three thinnest samples a simple correlation can be found between the energy of the peak and the stress induced by the trigonal distortion due to the epitaxial constraint on Si(111). Such a distortion measured by RBS and XRD on the same samples gives $\epsilon_t=3.5$, 3.2, and 2.4% for the 50, 62, and 350-Å sample, respectively, in good correlation with the measured phonon energies.

As far as the bandwidth is concerned, one needs to be more careful. We could argue that samples with coherent interfaces (i.e., the thinnest) should have a lower γ, and this is the case for the results obtained from the fits. On the other hand, the value of γ is sensitive to stress, inhomogeneities, defects and to the electron-phonon interaction and it is not always clear in which direction these effects act in a very thin layer. As mentioned above, the results for the thickest sample (890 Å) deviate considerably from the general trend found for all the others.

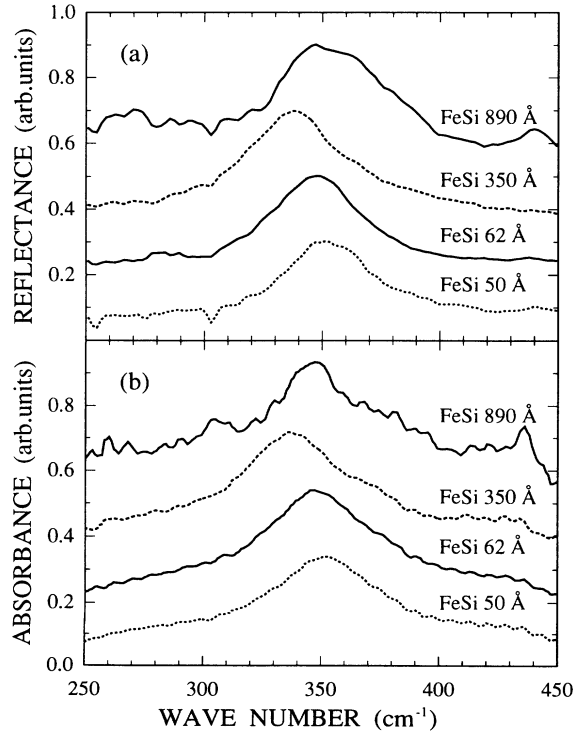

FIG. 2. Reflectance (a) and absorbance (b) results for FeSi films of different thicknesses, from 50 Å (at the bottom) to 890 Å (at the top).

IV. BRILLOUIN MEASUREMENTS

Brillouin scattering from long-wavelength surface acoustic waves (SAW's) was used to determine the whole set of elastic constants, c_{11}, c_{44}, and c_{12} of the FeSi films. The measurements were performed with the TM-

polarized 514-nm line of an argon laser at an incident power below 40 mW, in order to avoid excessive heating of the samples. The backscattered light was analyzed with a (3+3)-pass Fabry-Pérot tandem interferometer.[6] The scattering geometry was determined by the angle θ between the sample normal and the incoming wave vector $\mathbf{k}_0$ of the light. Due to the high optical absorption of the specimens, only the in-plane component of $\mathbf{k}_0$ was conserved and the in-plane wave vector $\mathbf{q}$ of the SAW, as sampled in the backscattering geometry, is given by $q=2k_0\sin\theta$. By adjusting the incidence angle between 30 and 70°, which is the experimentally accessible range, the length of the in-plane scattering vector $\mathbf{q}$ could be varied between 1.2 and 2.3×10^{-3} Å: This corresponds to a change in the acoustic penetration depth from 1000 to 3000 Å. In the case of thin films, the velocity of a SAW along a fixed direction on the surface (v_{SAW}) is a function of the elastic constants c_{ij}, the density of both substrate and film and the product qh (qh dispersion), where h is the film thickness. At fixed film configuration and thickness, it is possible to use the elastic continuum model described in Ref. 7 in order to fit v_{SAW} to the qh dispersion of our data (Fig. 3) with the c_{ij} as fitting parameters. In particular, by applying the Levenberg-Marquardt procedure for nonlinear least-squares fitting[8] it is possible to get simultaneously c_{11}, c_{44}, and c_{12} of the film alone, provided the elastic constants and density of the substrate along with the density of FeSi ($\rho=6550$ kg/m^2) are kept constant. On a (111)-oriented plane v_{SAW} is about 95% of the bulk shear velocity v_{shear} and the bulk velocity along the [1$\bar{1}$0] direction is given by $v^2_{\mathrm{shear}}=(1/(2\rho)(c_{11}-c_{12}))$.[7] Therefore, the SAW velocity is mainly dependent on the difference $c_{11}-c_{12}$, the shear modulus. This influences the fitting procedure in the following way: c_{11} or c_{12} alone have less weight on the fitted qh dispersion than the difference $c_{11}-c_{12}$. As a result, the uncertainty for c_{11} and c_{12} is typically around 8%, whereas it is 4% for $c_{11}-c_{12}$. In order to improve our accuracy also for c_{44}, we measured the dependence of v_{SAW} on the azimuthal angle in the (111) plane. This was achieved by rotating the sample around its surface normal and selecting SAW's propagating in different directions, at fixed length of the in-plane scattering vector. The dependence of v_{SAW} on azimuthal angle is called *angular dispersion*. Because of the sixfold symmetry, we varied the angle only from 0 to 30 degrees, starting from [1$\bar{1}$0]. The angular dispersion (see Fig. 4) was fitted by the same procedure as mentioned above. In Fig. 3 we report the qh dispersion for SAW's propagating along [1$\bar{1}$0] on two films with thicknesses of 350 and 890 Å, respectively. The velocities have been measured at five different values of the SAW wave vector for each film and no higher-order (*Sezawa*[7]) modes were detected. The negative slope of the qh dispersion of the surface acoustic mode indicates loading of the substrate, i.e., v_{SAW} on FeSi(CsCl) is lower than v_{SAW} on bare Si. For small values of qh the SAW is strongly coupled to the Si substrate and v_{SAW} is mainly determined by the elastic properties of the latter. As a consequence, the thinnest films (with $h=50$ and 62 Å) were not considered in the Brillouin measurements. Moreover, we performed a separate fit of the elastic con-

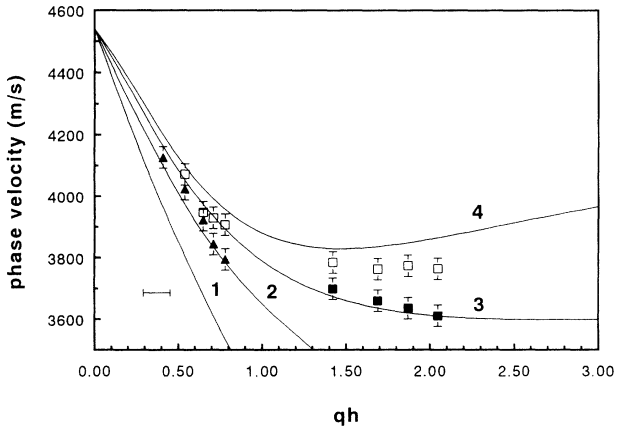

FIG. 3. qh dispersion of the surface acoustic mode measured on FeSi(111) films with the CsCl structure on Si(111) with thicknesses of $h_1=350$ Å (filled triangles, low-qh range) and $h_2=890$ Å (filled squares, high-qh range). The direction of propagation is [1$\bar{1}$0]. The open squares denote surface-acoustic-wave velocities on polycrystalline ϵ-FeSi films with the same thicknesses. The error bar for the velocity is in the range of 1–2 %. The horizontal error bar is due to the uncertainty in the film thickness of about 10%. The full curves 2 and 3 through the data points are the result of a fit yielding the elastic constants of Table I. Curve 1 is computed with the set of elastic constants estimated by our semiempirical method for $B=240$ GPa (Table I). Curve 4 was computed with the elastic constants for ϵ-FeSi (Ref. 10).

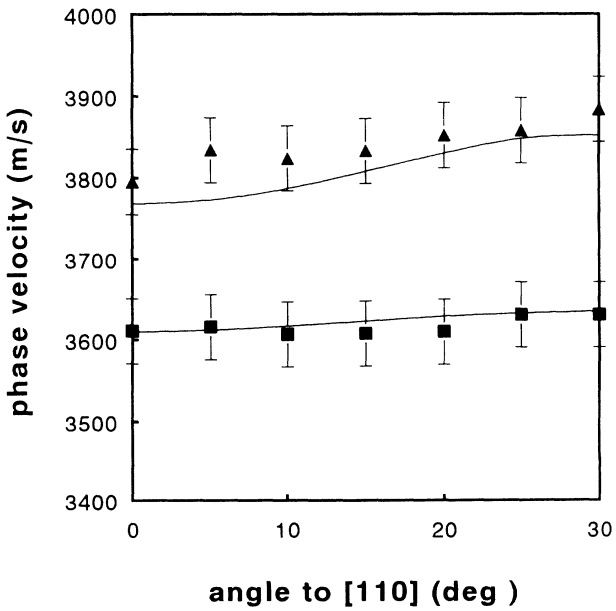

FIG. 4. Angular dispersion of SAW's propagating along the indicated directions on the 350- and the 890-Å film (filled triangles and filled squares, respectively). The full curves have been computed with the elastic constants described in the text and in Table I.

TABLE I. Theoretical elastic constants of FeSi with the CsCl structure and corresponding experimental results obtained by Brillouin scattering on thin films. B is the bulk modulus and η the anisotropy ratio (see text). (a) Estimate based on the experimental anisotropy ratio (b), while the Keating expression for semiconductors would give approximately 70. The c_{ij} and B are given in units of GPa.

Material	Structure	c_{11}	c_{44}	c_{12}	$c_{11}-c_{12}$	η	B	Ref.
FeSi (theory)	CsCl	313	41[a]	238	75	1.1[b]	263 (Refs. 1 and 17)	This work
FeSi (theory)	CsCl	291	42[a]	215	76	1.1[b]	240	This work
FeSi (350 Å)	CsCl	308±20	75±15	180±20	128±5	1.1	222	This work
FeSi (890 Å)	CsCl	322±20	108±15	128±20	194±5	1.1	192	This work
ϵ-FeSi	B20	306	131	16	290	0.9	112	10
CsCl		364	80	92	272	0.6	117	18

stants for the 350 and the 890-Å film, since the FIR measurements indicate that they are somehow different. The result of our fit are summarized in Table I. For these fits to the experimental data we chose c_{44} in such a way that the anisotropy constant $\eta=2c_{44}/(c_{11}-c_{12})$ was close to one (quasi-isotropic case), even if it is likely not to be the case for the sample wit $h=350$ Å, where the trigonal distortion is still not negligible. Anyhow, as mentioned above, the choice of c_{44} does not significantly influence the qh dispersion and plays a minor role.

For sake of comparison, the experimental qh dispersion obtained on polycrystalline ϵ-FeSi films is added in Fig. 3. In fact, both the $h_1=350$ Å and the $h_2=890$-Å-thick FeSi(CsCl) films were annealed at 350 °C and hence transformed to the polycrystalline ϵ-FeSi phase.[9] It is clearly seen that the presence of ϵ-FeSi leads to an increase of the SAW velocities due to the completely different elastic properties of this phase. In Fig. 3 we included also the calculated qh dispersion (solid line) by the elastic constants of ϵ-FeSi given in Ref. 10.

The FeSi (CsCl) c_{ij}'s for $h_1=350$ Å and $h_2=890$ Å provide corresponding v_{SAW} which fit equally well the experimental dispersion of Fig. 3 and the angular dispersion of Fig. 4 with $q=0.0023$ Å^{-1} (solid lines). The slight angular dependence of the velocity on the thinner film is mainly due to the elastic anisotropy of the underlying Si substrate which results in a sixfold symmetry of the angular dispersion[11,12] [the anisotropy ratio η for Si amounts to 1.56 (Ref. 7)]. For the thicker film the deviation from a constant value is within the measurement error of 1–2 % and indicates quasi-isotropy of the film itself, as should be expected for the bulk structure.

It is clear that the two sets of elastic constants for $h_1=350$ Å and $h_2=890$ Å differ and that by increasing film thickness a trend in $c_{11}-c_{12}$ and the bulk modulus is present towards the corresponding values for ϵ-FeSi (see Table I). In Sec. III we have already see that the vibrational properties of the $h_2=890$-Å film do not follow the general trend for the CsCl structure. In order to resolve this apparent ambiguity theoretical support is needed, which is able to correlate and interpret the data for the vibrational and the elastic properties.

V. CALCULATION PROCEDURE

The calculation procedure that we adopted in the present work has been described in detail in a recent publication by two of us, concerning the elastic properties of $NiSi_2$, $CoSi_2$, and $FeSi_2$.[13] It is based on the partition of the total energy into a band-structure contribution and a repulsive potential. The former is calculated as a summation of semiempirical, tight-binding (TB) electronic states up to the current Fermi energy. The latter is an exponential two-body function, which takes into account the quantum-mechanical repulsion of the electronic orbitals[14]

$$U_{rep}=\phi \exp\left[-\alpha\frac{d}{d_0}\right], \tag{1}$$

where d_0 is the Fe-Si equilibrium distance. Total-energy variations corresponding to frozen-phonon displacement patterns and to elastic deformations are estimated by scaling the TB Slater-Koster parameters[15] with Harrison's universal laws[16] and by explicitly introducing the actual atomic positions into the analytic repulsive potential, which is summed up to the second-nearest neighbors. The TB parameters (see Table II), which include Fe-Fe interactions, have been found by fitting the TB band structure onto the one obtained by a self-consistent full-potential linearized augmented plane-wave (FLAPW) calculation.[1,17] The two repulsive parameters (α,ϕ) are estimated by imposing equilibrium and stability conditions on the total energy and by using the experimental lattice constant a and the FLAPW bulk modulus B (Ref. 17) (Table III). In short, this method can be considered as an interpolation of *ab initio* results, which, however, turns out to be much more flexible and computer-time saving than the self-consistent total-energy calculations. In Fig. 5 we display the cohesion-energy curve for isotropic volume deformation, as calculated by our semiempirical method (solid line). Open circles are the FLAPW results and we see that the agreement is very good. Elastic constants, c_{11} and c_{12}, are readily evaluated by the energy variation ΔE^{el}, corresponding to a suitable rectangular deformation of the xz plane, with no relaxation along the y axis ($x\rightarrow x+\delta, z\rightarrow z-\delta, y\rightarrow y$) (Ref. 13)

$$c_{11}=B+\frac{2\Delta E^{el}}{3V_0\delta^2} \tag{2}$$

$$c_{12}=B-\frac{\Delta E^{el}}{3V_0\delta^2}\ . \tag{3}$$

TABLE II. TB parameters for FeSi in the CsCl structure (eV), where d is the interatomic distance.

	d (Å)	$ss\sigma$	$sp\sigma$	$pp\sigma$	$pp\pi$	$sd\sigma$	$pd\sigma$	$pd\pi$	$dd\sigma$	$dd\pi$	$dd\delta$
Fe-Si	2.35	−1.08	1.33	1.46	−0.71						
Si-Fe	2.35	−1.08	1.09	1.46	−0.71	−1.20	−1.09	0.74			
Si-Si	2.72	−0.89	1.44	2.54	−1.02						
Fe-Fe	2.72								−0.69	0.25	0.07
		$E(s)$	$E(p)$	$E(d)$							
Fe		5.16	6.45	−1.92							
Si		−5.44	2.52								

The estimation of c_{44} is not straightforward in our procedure, since relaxation of atomic positions is here involved,[13] so that we evaluated it by assuming the same anisotropy parameter of the Brillouin fit ($\eta=1.1$). Our results are reported in Table I.

The frozen-phonon distortion-energy $\Delta E^{\rm ph}$, corresponding to the TO mode at the Γ point, is evaluated for a counterphase motion of Fe and Si atoms with the center of mass at rest and no change of the cubic unit cell. The phonon frequency ω and the anharmonicity contributions (if any) are then given by

$$\Delta E^{\rm ph}=\sum_s \frac{1}{2}M_s\omega^2 u_s^2+\sum_s 4\kappa\left[\frac{u_s}{\sqrt{3}}\right]^3+\mathcal{O}(u^4)\,, \qquad (4)$$

where the sum runs over atoms s=Fe, Si, and $M_{\rm Fe}\mathbf{u}_{\rm Fe}=-M_{\rm Si}\mathbf{u}_{\rm Si}$ with $\mathbf{u}_s$ along ⟨111⟩, and no cubic anharmonicity is present in this case ($\kappa=0$). By using the FLAPW estimation of B (263 GPa) our evaluation of the TO frequency (346 cm^{-1}) is slightly higher than the experimental finding for the low-stress situation (335 cm^{-1}). Such overestimation of the optical frequency on the basis of the bulk modulus fitting could be a physiologic feature of the TB method, still, in our case, the input value of B is not experimental and an overestimation up to 10% is not uncommon in first-principle predictions. Therefore it could be more safe to adjust the input value of B in such a way that the best agreement with the experimental TO frequency is obtained (somehow a frequency fitting) and to use it for complementary calculation of the elastic constants. In fact, if we lower B by 10% (240 GPa), we obtain an estimation of ω_0, which is well within the experimental error for the FIR data (332 cm^{-1}, see Table III). The elastic constants calculated with this bulk modulus are also displayed in Table I, but no significant change is found with respect to the key quantity $c_{11}-c_{12}$. We have finally estimated the frozen-phonon frequency of the longitudinal-acoustic (LA) vibration at the Brillouin-zone boundary, along the [111] direction (R point), which is degenerate by symmetry with the transverse-acoustic (TA) frequency. It turns out to be 156 cm^{-1} for $B=240$ GPa. Our accuracy, however, is lower than the one for the prediction of the TO phonon at Γ, due to the larger fluctuations in the $\Delta E^{\rm ph}(u_{\rm Fe})$ curve, which we interpolate by a polynomial function.[13] The theoretical estimation of $v_{\rm shear}$ along [111], as deduct by a sine-like fitting of the TA dispersion along this direction, turns out to be 2461 m/s, in good agreement with $v_{\rm shear}$ in the (111) plane (2409 m/s), as calculated by $[1/(2\rho)(c_{11}-c_{12})]$. This feature is expected for nearly isotropic materials, so that consistency between frozen phonon estimation and elastic constant results is also confirmed.

TABLE III. Repulsive parameters ϕ and α, along with the input values for a_0 and B, and calculated frequency of the TO phonon at the Γ points.

	a_0 (Å)	B (GPa)	ϕ (keV)	α	ω (cm^{-1})
FeSi	2.77	263 (Ref. 1)	2.79	7.84	346
FeSi	2.77	240	2.09	7.53	332

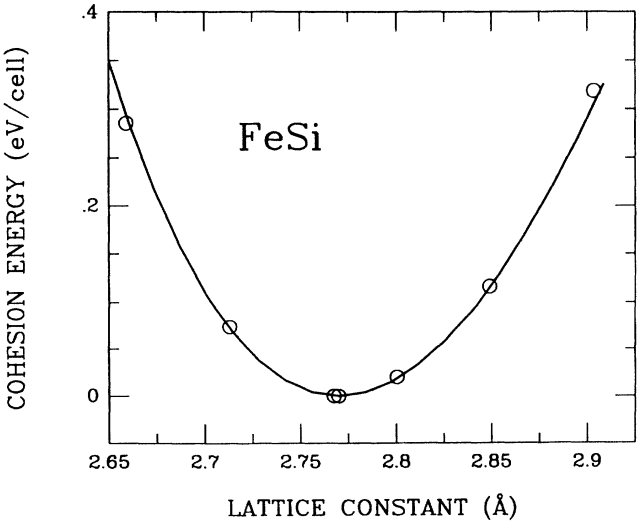

FIG. 5. Cohesion energy as a function of the lattice constant. Solid line is the TB calculation, open circles are FLAPW results.

VI. DISCUSSION AND CONCLUSIONS

We have seen that the experimental IR transmittance and reflectance measurements provide a broad vibrational peak (identified with the TO mode) which shifts to higher frequency with increasing strain in the film. Although the strain is actually biaxial, its hydrostatic component $\frac{1}{3}\mathrm{Tr}\underline{\epsilon}=\frac{1}{3}(2\epsilon_{\parallel}+\epsilon_{\perp})$ corresponds to nearly 1% compression when moving from the 350-Å sample to the 62-Å one and the relative shift in TO frequency is 13 cm^{-1}. This is in quantitatively confirmed by our calculations, since we obtain an increase of 11–24 cm^{-1} for the TO frequency, by introducing an isotropic compression of the lattice parameter by 1–2 %, respectively. Taking for granted the lowering of the frequency with strain relaxation and, in turn, with sample thickness, the increase for the 890-Å film seems to indicate that some effect other than strain relaxation is taking place in this sample. We have performed x-ray measurements on one piece of the 890-Å sample (as-grown) and on another one which was annealed just at 200 °C (well below the transition temperature in the ordinary, thinner films). The same thing was done for the 350-Å sample. In the latter case the intensity of the CsCl peaks decreased in the annealed portion by no more than 20%, which means that by large the structure does survive. The 890-Å sample, however, is completely transformed by the annealing, since almost the entire intensity of the CsCl peaks vanishes. Actually, we discovered something even more interesting, i.e., the trigonal distortion of the 890-Å sample to be lower than the 350-Å one not because $\epsilon_{\parallel}$ is smaller (relaxation), but $(\epsilon_{\parallel}-\epsilon_{\perp})$ is smaller and the hydrostatic component is larger. Probably, an isotropic compression sets in, which drives the lattice parameter towards the silicon one $(\epsilon_{\parallel}\simeq\epsilon_{\perp})$. This explains the higher vibrational frequency, which increases with compression.

By considering the experimental elastic constants derived from the SAW data for the 890-Å sample (see Table I and Fig. 3), we find a big discrepancy with the theoretical evaluation of c_{12}, both for $B=263$ GPa and $B=240$ GPa. On the other hand, the experimental data give rise to a B value of 192 GPa (Table I), which is much below the one predicted by the FLAPW calculation and well outside the estimated error of the local-density approximation employed in the FLAPW method. Thus, we used our theoretical set of elastic constants for $B=240$ GPa as input parameters for the calculation of the dispersion relation of v_{SAW}. The resulting curve (labeled by 1) is also shown in Fig. 3. We note that the experimental data for the 350-Å sample, visible at small qh, are closer to the theoretical dispersions and this is evident also by inspection of the corresponding values for the elastic constants (Table I). The discrepancy between the two is probably due to residual strain effects in the 350-Å sample, which is not completely free from biaxial compression, but the values for the 890-Å sample are really far off. By considering the elastic constants and the bulk modulus of the ϵ phase (Table I), we note that the corresponding values for the 890-Å sample are shifted towards these characteristic values (small c_{12} and small B).

On the other hand, it is fair to stress that the results of the structural characterization do not give direct evidence for a modification of the crystal structure of the 890-Å sample, even if it turns out to be clearly not homogeneous. The RBS minimum channeling yield of 8.9% found for the [111] direction and the intensity of the room-temperature x-ray diffraction peaks, even if broadened, seem to rule out the possibility that a large portion of the film has undergone the phase transition. Plan-view transmission electron microscopy confirmed the CsCl structure to be present in more than 90% of the film area. It is not clear if the few grains of γ-$FeSi_2$ found by this method are an artifact of the thinning procedure. Moreover, the temperature dependence of the electrical resistivity indicates no substantial deviation from the behavior found for the 350-Å film, as could be attributed to a change of the crystal structure.[19] The question now remains: What happens in the thickest sample, where an isotropic compression sets in which affects the vibrational frequency and the elastic constants? The origin of such effect could be addressed, in our opinion, to the homogeneously dispersed appearance of ϵ-phase micrograins (less than 10% with respect to the CsCl phase), which display a larger volume per atom (11.16 and 10.28 Å^3, respectively), so that isotropic compression is generated. This *nanophase* configuration could explain the broadening of room-temperature x-ray peaks, the satellite peaks in the FIR spectra (actually a local probe) and the shift of the elastic constants (a mesoscopic information) towards the ϵ-phase values. As the sample is annealed, we envisage the micrograin size to grow up to the polycrystalline configuration of the ϵ phase. This view is supported by the dispersion relation of v_{SAW} for polycrystalline FeSi in the ϵ phase (Fig. 3), which lies above that of the 890-Å sample.

Obviously, this is just a speculation. More theoretical and experimental studies will be required in order to work out the actual situation of pseudomorphic FeSi samples at the upper limits of film thickness, somehow well beyond the usual range of substrate-originated stablization.

ACKNOWLEDGMENTS

We are indebted to Hansruedi Deller (ETH, Zürich) for communicating his TEM observations and to Camilla Calegari (University of Milano) for helpful discussions. Financial support by the Commission of the European Communities (SCIENCE Plan) and by the Fondation Suisse pur la Recherche en Microtechnique is gratefully acknowledged.

*Present address: Department of Physics, Colorado State University, Fort Collins, CO 80523.

†Present address: National Renewable Energy Laboratory, 1617 Cole Boulevard, Golden, CO 80401-3393.

[1] H. von Känel, K. A. Mäder, E. Müller, N. Onda, and H. Sirringhaus, Phys. Rev. B **45**, 13 807 (1992).

[2] H. von Känel, R. Stalder, H. Sirringhaus, N. Onda, and J. Henz, Appl. Surf. Sci. **53**, 196 (1991).

[3]D. M. Wood and A. Zunger, Phys. Rev. B **40**, 4062 (1989).
[4]R. Bruinsma and A. Zangwill, J. Phys. (Paris) **47**, 2055 (1986).
[5]N. Onda, H. Sirringhaus, S. Goncalves-Conto, C. Schwarz, E. Müller-Gubler, and H. von Känel, in *Evolution of Surface and Thin Film Microstructures,* edited by H. A. Atwater, E. Chason, M. Grabow, and M. Lagally, MRS Symposia Proceedings No. 280 (Materials Research Society, Pittsburgh, 1993).
[6]J. R. Sandercock, Solid State Commun. **26**, 547 (1978).
[7]G. W. Farnell, in *Physical Acoustics,* edited by W. P. Mason and R. N. Thurston (Academic, New York, 1970), Vol. 6, p. 109.
[8]W. H. Press, B. Flannery, S. A. Teukolsky, and W. T. Vetterling, *Numerical Recipes* (Cambridge University Press, Cambridge, England, 1989), p. 498.
[9]H. von Känel, N. Onda, H. Sirringhaus, E. Müller-Gubler, S. Goncalves-Conto, and C. Schwarz, Appl. Surf. Sci. **70/71**, 559 (1993).
[10]G. P. Zinoveva, L. P. Andreeva, and P. V. Geld, Phys. Status Solidi A **23**, 711 (1974).
[11]M. W. Elmiger, J. Henz, H. von Känel, M. Ospelt, and P. Wachter, Surf. Interface Anal. **14**, 18 (1989).
[12]M. Mendik, S. Sathish, A. Kulk, G. Gremaud, and P. Wachter, J. Appl. Phys. **71**, 2830 (1992).
[13]G. Malegori and L. Miglio, Phys. Rev. B **48**, 9223 (1993).
[14]J. A. Majewski and P. Vogl, in *The Structures of Binary Compounds,* edited by F. R. de Boer and D. G. Pettifor (North-Holland, Amsterdam, 1989), p. 287.
[15]J. C. Slater and G. F. Koster, Phys. Rev. **94**, 1498 (1954).
[16]W. A. Harrison, *Electronic Structure and the Properties of Solids* (Freeman, San Francisco, 1980).
[17]K. A. Mäder, H. von Känel, and A. Baldereschi, Phys. Rev. B **48**, 4364 (1993).
[18]G. Simmons and H. Wang, *Single Crystal Elastic Constants and Calculated Aggregate Properties* (MIT, Cambridge, MA, 1971), p. 19.
[19]N. Onda, H. Sirringhaus, P. Steiner, and H. von Känel, *Evolution of Surface and Thin Film Microstructures* (Ref. 5).